

Titanium Nitride Films for Ultrasensitive Microresonator Detectors

Henry G. Leduc,¹ Bruce Bumble,¹ Peter K. Day,¹ Byeong Ho Eom,² Jiansong Gao,³ Sunil Golwala,² Benjamin A. Mazin,⁴ Sean McHugh,⁴ Andrew Merrill,⁴ David C. Moore,² Omid Noroozian,² Anthony D. Turner,¹ and Jonas Zmuidzinas²

¹*Jet Propulsion Laboratory, California Institute of Technology, Pasadena, CA 91109*

²*Division of Physics, Mathematics, and Astronomy, California Institute of Technology, Pasadena, CA 91125*

³*National Institute of Standards and Technology, Boulder, CO, 80305*

⁴*Department of Physics, University of California, Santa Barbara CA 93106-9530*

(Dated: 8 October 2018)

Titanium nitride (TiN_x) films are ideal for use in superconducting microresonator detectors because: a) the critical temperature varies with composition ($0 < T_c < 5$ K); b) the normal-state resistivity is large, $\rho_n \sim 100 \mu\Omega \text{ cm}$, facilitating efficient photon absorption and providing a large kinetic inductance and detector responsivity; and c) TiN films are very hard and mechanically robust. Resonators using reactively sputtered TiN films show remarkably low loss ($Q_i > 10^7$) and have noise properties similar to resonators made using other materials, while the quasiparticle lifetimes are reasonably long, $10 - 200 \mu\text{s}$. TiN microresonators should therefore reach sensitivities well below $10^{-19} \text{ W Hz}^{-1/2}$.

PACS numbers: 07.57.Kp, 03.67.Lx, 74.25.nm, 85.25.Oj, 85.25.Pb

Keywords: superconducting detectors, resonators

Absorption of photons with $h\nu \geq 2\Delta \approx 3.5 k_B T_c$ in a superconductor breaks Cooper pairs into electrons or "quasiparticles", producing a perturbation $\delta\sigma(\omega) = \delta\sigma_1(\omega) - j\delta\sigma_2(\omega)$ of the complex conductivity.¹⁻³ Such perturbations may be readily sensed through vector microwave measurements of lithographed microresonators, and frequency multiplexing enables large detector arrays.^{4,5} These devices are commonly known as microwave kinetic inductance detectors, or MKIDs because the inductive (frequency shift) signal is considerably larger ($\beta = \delta\sigma_2/\delta\sigma_1 \sim 3$). However, the dissipation signal can be more sensitive,⁶ especially at lower modulation frequencies, because the resonator frequency exhibits $1/f^{1/2}$ noise⁵⁻⁸ caused by a surface distribution of two-level system (TLS) fluctuators.^{6,9-12} In this letter, we discuss the requirements for ultrasensitive MKIDs and show that they are very well fulfilled by the measured properties of titanium nitride (TiN) films.

For dissipation readout using the standard shunt-coupled, forward transmission (S_{21}) configuration⁵, the amplifier contribution to the noise equivalent power (NEP) is given by

$$\text{NEP}_{\text{diss}}^{(\text{amp})} = 2 \frac{N_{\text{qp}} \Delta}{\eta_{\text{opt}} \tau_{\text{qp}}} \sqrt{\frac{k_B T_{\text{amp}}}{\chi_c \chi_{\text{qp}} P_{\text{read}}}}. \quad (1)$$

Here N_{qp} is the number of quasiparticles in the detector active volume V_{sc} ; $\eta_{\text{opt}} \approx 0.7$ is the efficiency with which photon energy is converted to quasiparticles;⁵ τ_{qp} is the quasiparticle lifetime; T_{amp} is the amplifier noise temperature; P_{read} is the microwave readout power absorbed by the quasiparticles; $\chi_c = 4Q_r^2/Q_c Q_i \leq 1$ is optimized by matching the coupling and internal quality factors $Q_c = Q_i$ to give a resonator quality factor $Q_r^{-1} = Q_c^{-1} + Q_i^{-1} = 2Q_i^{-1}$; and $\chi_{\text{qp}} = Q_i/Q_{i,\text{qp}} \leq 1$ is the fraction of the resonator's internal dissipation that is

due to resistive quasiparticle losses (σ_1). In terms of the microwave generator power P_{gen} incident on the feedline, $P_{\text{read}} = \chi_c \chi_{\text{qp}} P_{\text{gen}}/2$. For frequency readout, the amplifier NEP is reduced by a factor of β ; however, TLS noise may then be an issue. Note that equation (1) does not include the transmission of the optical system or the absorption efficiency of the detector.

For minimizing the amplifier NEP, P_{read} should be chosen so that the microwave and optical quasiparticle generation rates are about equal, provided that the optical loading is high enough that the quasiparticle dissipation dominates ($\chi_{\text{qp}} \rightarrow 1$). In this case, amplifier noise temperatures of order $T_{\text{amp}} \sim 1-10$ K are sufficient to achieve the photon noise limit in the mm/submm/far-infrared bands.¹¹ In this letter we are primarily concerned with the lowest NEP values achievable, so we examine the opposite limit of vanishingly small optical power and a correspondingly small quasiparticle population. Other dissipation mechanisms (radiation, TLS, grain boundaries, etc.) will then limit the resonator quality factor to some maximum value $Q_{i,\text{max}}$, so $\chi_{\text{qp}} \propto N_{\text{qp}} \rightarrow 0$. Also, the quasiparticle lifetime is observed¹³⁻¹⁵ to reach a maximum value τ_{max} for densities $n_{\text{qp}} = N_{\text{qp}}/V_{\text{sc}} \lesssim 100 \mu\text{m}^{-3}$. If thermally generated quasiparticles are made insignificant by cooling and other sources of stray power are eliminated,¹⁶ readout power dissipation remains as the only source of quasiparticles, which are generated with some efficiency $\eta_{\text{read}} = N_{\text{qp}} \Delta / P_{\text{read}} \tau_{\text{max}} \leq 1$. Eqn. (1) then yields

$$\text{NEP}_{\text{diss}}^{(\text{amp})} \geq \frac{2}{\eta_{\text{opt}}} \sqrt{\frac{2\eta_{\text{read}} N_0 \Delta^2 V_{\text{sc}} k_B T_{\text{amp}}}{\chi_c \alpha_{\text{sc}} S_1(\omega, T) \tau_{\text{max}} Q_{i,\text{max}}}}. \quad (2)$$

Here $\alpha_{\text{sc}} \leq 1$ is the kinetic inductance fraction,⁵ S_1 is a dimensionless Mattis-Bardeen factor of order unity,^{11,17} and N_0 is the single-spin density of states at the Fermi

energy. Thus, $\mathcal{F} = \alpha_{sc}\tau_{max}Q_{i,max}/N_0V_{sc}$ is a useful figure of merit. In addition, the gap parameter Δ plays a crucial role: $NEP_{diss}^{(amp)} \propto \Delta^2$ because $\tau_{max}^{-1} = n_{qp}^*R \propto n_{qp}^*\Delta^2$. We will show that \mathcal{F} for TiN is considerably better than for other materials explored to date.

Although good resonators can be made with $T_c \approx 15$ K NbTiN films,^{8,18} lower- T_c materials are needed for sensitive detectors. We therefore studied TiN_x films produced by reactive magnetron sputtering onto ambient-temperature, 100 mm diameter, high resistivity (> 10 k Ω cm) (100) HF-cleaned silicon substrates. The titanium sputtering target was 99.995% pure, and the sputtering gases (N₂ and Ar) were 99.9995% pure. As shown in Fig. 1, the TiN film T_c is sensitive to composition.¹⁹ Microresonator structures were fabricated using deep UV projection lithography followed by inductively coupled plasma etching using a chlorine chemistry (BCl₃/Cl₂). Both distributed coplanar waveguide (CPW) resonators^{5,6} as well as lumped-element resonators²⁰ with meandered inductors and interdigitated capacitors (see Fig. 2) were produced.

For our TiN films with 0.7 K $\leq T_c \leq 4.5$ K and 20 nm $\leq t \leq 100$ nm, the normal-state resistivity was typically $\rho_n \approx 100$ $\mu\Omega$ cm, with $\rho_n(300$ K)/ $\rho_n(4$ K) ≈ 1.1 . This resistivity is similar to polycrystalline TiN films reported in the literature but considerably higher than for

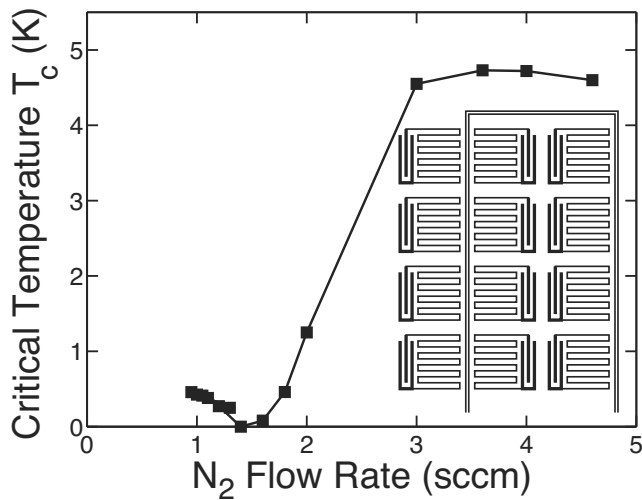


FIG. 1. The critical temperature of reactively sputtered TiN films as a function of the N₂ flow rate. The Ar flow rate was set to 15 sccm and the total pressure to 2 mTorr. The deposition rate was 35 nm/min using 1 kW DC power, a 150 mm diameter Ti target, and a target to substrate distance of 15 cm. The flow for both gases was set by thermal mass flow controllers, while the pressure in the 17.5 L sputtering chamber was maintained by adjusting the pump rate using a closed-loop system consisting of a capacitance manometer, a butterfly-type throttle valve, and a feedback controller. The inset provides a schematic illustration of the geometry of the 14 \times 16 close-packed resonator array, with dark regions representing TiN metallization.

single-crystal films.²¹ The high resistivity (relative to Al, Ta, or Nb) is very convenient for obtaining highly efficient far-infrared photon absorption in lumped-element resonator structures.²⁰ As a consequence of the Mattis-Bardeen relationship $L_s \approx \hbar R_s/\pi\Delta$ between the normal-state surface resistance R_s and the superconducting surface inductance L_s , the large resistivity also guarantees a large kinetic inductance fraction $\alpha_{sc} \rightarrow 1$.

Fig. 2b shows a lumped-element 1.5 GHz TiN resonator consisting of a meandered inductor and an interdigitated capacitor (IDC), designed to serve as a ~ 1 mm² pixel in a 14 \times 16 far-IR imaging array that is read out using a single coplanar strip (CPS) feedline. The array and feedline geometry is shown schematically in the inset to Fig. 1; the spacing between pixels is around 60 μ m. The IDC consists of four 0.9 mm \times 10 μ m vertical strips with relatively large 10 μ m gaps to reduce noise and dissipation¹², while the inductor consists of 32 1 mm \times 5 μ m horizontal strips and has $V_{sc} \approx 5900$ μ m³ and $\alpha_{sc} \approx 0.74$. Experiments using a cryogenic blackbody source and a metal-mesh, 215 μ m wavelength bandpass filter verify the basic functionality of these devices and show that the meander is an efficient single-polarization absorber.

Although the resonators were predicted to have $Q_c^* = 1.7 \times 10^6$, the measured Q_c values for the array show a very large scatter $0.002 < Q_c/Q_c^* < 6$, which is largely due to unanticipated multi-resonator modes arising from pixel-pixel coupling. Indeed, electromagnetic simulations show that two isolated, identically tuned, nearest-neighbor pixels would produce symmetric and antisymmetric coupled modes with a frequency splitting of ~ 100 MHz, so the interpixel coupling is much larger

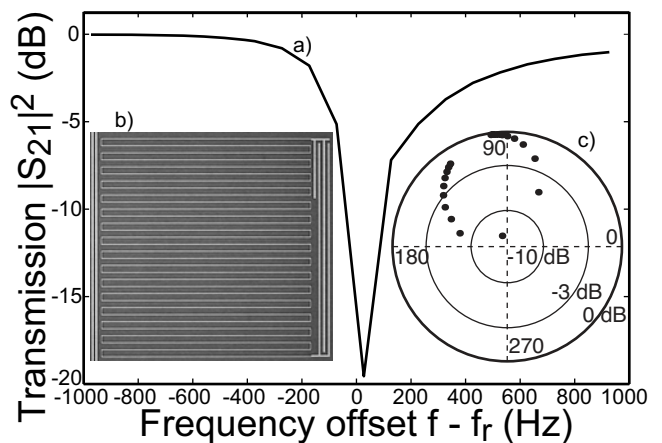


FIG. 2. a) deep resonance measured at $T = 100$ mK and $P_{gen} = -90$ dBm with $f_r = 1.53$ GHz, $Q_r = 3.6 \times 10^6$, and $Q_i = 3 \times 10^7$. The device was a 16 \times 14 close-packed array of lumped-element resonators made using a $t = 40$ nm TiN film with $T_c = 4.1$ K, $R_s = 25$ Ω , and $L_s = 8.4$ pH. In addition, six resonances with $Q_i > 2 \times 10^7$ were seen, and ≥ 50 had $Q_i > 10^7$. The image (b) shows a single 1 mm² lumped-element resonator. The polar S_{21} plot (c) clearly shows the expected resonance loop.

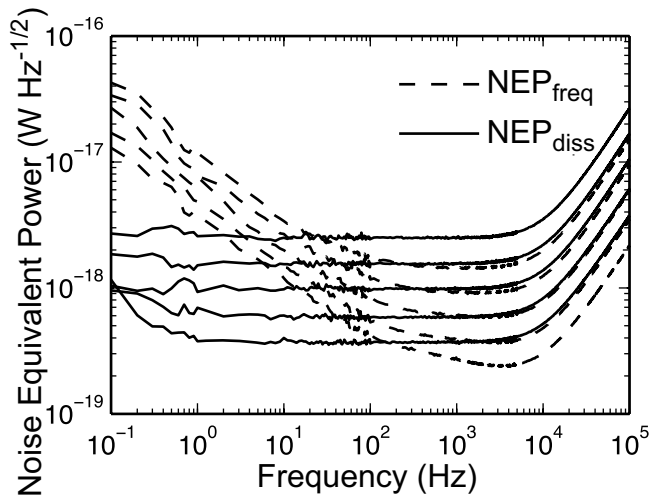


FIG. 3. NEP for frequency readout (dashed lines) and dissipation readout (solid lines) measured for a $t = 20$ nm, $T_c = 1.1$ K TiN CPW resonator, for readout powers $P_{\text{gen}} = -113, -109, -105, -101,$ and -97 dBm (top to bottom). The resonator center strip is $3 \mu\text{m}$ wide and 4.5 mm long, and has a $2 \mu\text{m}$ gap to ground, giving $V_{\text{sc}} = 270 \mu\text{m}^3$ and $\alpha_{\text{sc}} = 0.95$. Transmission (S_{21}) data measured at $T = 52$ mK and $P_{\text{read}} = -93$ dBm give $f_r = 5.380$ GHz, $Q_r = 3.2 \times 10^4$, and $Q_i = 10^5$. This resonance is the 3rd harmonic of the fundamental at 1.794 GHz, which was also observed but lies below the amplifier's 4-12 GHz band. Microwave pulse experiments and cosmic ray events indicate $\tau_{\text{max}} = 100 \mu\text{s}$ at $P_{\text{gen}} = -109$ dBm, consistent with τ_{max} values seen in photon detection experiments with other 1.1 K TiN devices.

than the ~ 1 MHz intended resonator frequency spacing. We have since developed improved pixel designs and filled arrays with dramatically reduced coupling; these results will be reported in a future publication. However, the very large accidental Q_c values have fortunately enabled a deep probe of the microwave loss of TiN. As shown in Figs. 2a and 2c, the measurements imply $Q_{i,\text{max}}(\text{TiN}) \geq 3 \times 10^7$. The interpretation of $Q_{i,\text{max}}$ of the coupled modes is secure since all resonances displayed the same frequency vs. temperature curve and follow the Mattis-Bardeen prediction. Furthermore, the improved uncoupled resonators also show $Q_i > 10^7$. Regarding lower- T_c material, to date our results indicate that $Q_{i,\text{max}} > 5 \times 10^6$ for 0.85 K TiN; higher- Q_c resonators will be needed to push this limit. The best Al or Nb resonators to date have $Q_{i,\text{max}}(\text{Al}) \sim 2 \times 10^6$; however, for such high Q one must generally use thick films ($t \geq 100$ nm) for which $\alpha_{\text{sc}} \sim 0.05$.¹¹ Therefore, $\alpha_{\text{sc}} Q_{i,\text{max}}(\text{TiN}) \geq 2 \times 10^7$ whereas $\alpha_{\text{sc}} Q_{i,\text{max}}(\text{Al}, \text{Nb}) \sim 10^5$. We will consider the remaining factors in \mathcal{F} below.

For ease of comparison to previous measurements, we studied the noise of a coplanar waveguide resonator with our standard geometry (see Fig. 3 for details). After correcting for the higher (200Ω) characteristic impedance and third-harmonic operation for the TiN CPW device¹¹, the measured frequency noise

($S_f(1 \text{ kHz}) \approx 3 \times 10^{-19} \text{ Hz}^2/\text{Hz}$ at $P_{\text{gen}} = -97$ dBm) may be compared to other resonators operated at internal power $P_{\text{int}} = -55$ dBm, and is about a factor of two lower than typically seen.⁶ This result, along with the very similar spectral shape and power dependence, implies that the frequency noise of the TiN device almost certainly arises from surface TLS fluctuators. As with other materials, no dissipation fluctuations are seen above the cryogenic amplifier noise floor. The corresponding electrical NEP is $4 \times 10^{-19} \text{ W Hz}^{-1/2}$ at 1 Hz even though $Q_c \approx 4 \times 10^4$ is quite modest. A smaller-volume resonator with $Q_c > 10^6$ should give an NEP in the few $10^{-20} \text{ W Hz}^{-1/2}$ range.

For calculating NEP, it is necessary to assume a value for the electronic density of states N_0 . The results of Dridi *et al.*²² are insensitive to stoichiometry over our range of interest¹⁹ and correspond to $N_0 = 8.7 \times 10^9 \text{ eV}^{-1} \mu\text{m}^{-3}$ including the electron-phonon enhancement factor $1 + \lambda$,^{23,24} or about a factor of two lower than for Al. However, recent work²⁵ has indicated that electron correlation effects in TiN may reduce N_0 ; if so this would lower the NEP. Detection experiments with TiN resonators should help elucidate this issue.

Another important factor is the quasiparticle lifetime. From far-IR, UV, and X-ray photon detection experiments, we find lifetimes of $\tau_{\text{max}} \approx 15 \mu\text{s}$ for $T_c = 4$ K material, $100 \mu\text{s}$ for $T_c = 1.1$ K, and $200 \mu\text{s}$ for $T_c = 0.8$ K, scaling roughly as T_c^{-2} as might be expected. For $T_c = 1.1$ K, the lifetime is in the range seen for thin Al ($t = 20 - 40$ nm) films but is an order of magnitude shorter than the best thick ($t > 100$ nm) Al films.¹⁵

Thus, the remaining factors $\tau_{\text{max}}/N_0 V_{\text{sc}}$ contained in \mathcal{F} are about the same for TiN, thin Al, and thick Al, to within a factor of two. Therefore, the two orders of magnitude advantage in $\alpha_{\text{sc}} Q_{i,\text{max}}$ for TiN translates directly into a factor of 10 improvement in sensitivity, or for applications requiring large sensors, an improvement of two orders of magnitude in device area. Furthermore, the ability to reach high Q_r with TiN resonators should enable very dense MKID frequency multiplexing, and should also be of considerable interest for quantum information and other applications.

This research was carried out in part at the Jet Propulsion Laboratory (JPL), California Institute of Technology, under a contract with the National Aeronautics and Space Administration. The devices used in this work were fabricated at the JPL Microdevices Laboratory. This work was supported in part by the NASA Science Mission Directorate, JPL, and the Gordon and Betty Moore Foundation.

¹N. Bluzer, J. Appl. Phys., **78**, 7340 (1995).

²A. M. Gulian and D. Van Vechten, Appl. Phys. Lett., **67**, 2560 (1995).

³A. V. Sergeev and M. Y. Reizer, Int. J. Mod. Phys. B, **10**, 635 (1996).

⁴B. A. Mazin, P. K. Day, J. Zmuidzinas, and H. G. LeDuc, AIP Conf. Proc., **605**, 309 (2002).

⁵P. Day, H. G. LeDuc, B. A. Mazin, A. Vayonakis, and J. Zmuidzinas, Nature, **425**, 817 (2003).

- ⁶J. Gao, J. Zmuidzinas, B. A. Mazin, H. G. Leduc, and P. K. Day, *Appl. Phys. Lett.*, **90**, 102507 (2007).
- ⁷B. A. Mazin, Ph.D. thesis, California Institute of Technology, Pasadena CA (2004).
- ⁸R. Barends, H. L. Hortensius, T. Zijlstra, J. J. A. Baselmans, S. J. C. Yates, J. R. Gao, and T. M. Klapwijk, *IEEE Trans. Appl. Supercond.*, **19**, 936 (2009).
- ⁹S. Kumar, J. Gao, J. Zmuidzinas, B. A. Mazin, H. G. Leduc, and P. K. Day, *Appl. Phys. Lett.*, **92**, 123503 (2008).
- ¹⁰J. Gao, M. Daal, J. M. Martinis, A. Vayonakis, J. Zmuidzinas, B. Sadoulet, B. A. Mazin, P. K. Day, and H. G. Leduc, *Appl. Phys. Lett.*, **92**, 212504 (2008).
- ¹¹J. Gao, Ph.D. thesis, California Institute of Technology, Pasadena CA (2008).
- ¹²O. Noroozian, J. Gao, J. Zmuidzinas, H. G. Leduc, and B. A. Mazin, *AIP Conf. Proc.*, **1185**, 148 (2009).
- ¹³R. Barends, J. J. A. Baselmans, S. J. C. Yates, J. R. Gao, J. N. Hovenier, and T. M. Klapwijk, *Phys. Rev. Lett.*, **100**, 257002 (2008).
- ¹⁴A. G. Kozorezov, A. A. Golubov, J. K. Wigmore, D. Martin, P. Verhoeve, R. A. Hijmering, and I. Jerjen, *Phys. Rev. B*, **78**, 174501 (2008).
- ¹⁵R. Barends, S. van Vliet, J. J. A. Baselmans, S. J. C. Yates, J. R. Gao, and T. M. Klapwijk, *Phys. Rev. B*, **79**, 020509 (2009).
- ¹⁶J. M. Martinis, M. Ansmann, and J. Aumentado, *Phys. Rev. Lett.*, **103**, 097002 (2009).
- ¹⁷D. C. Mattis and J. Bardeen, *Phys. Rev.*, **111**, 412 (1958).
- ¹⁸R. Barends, H. L. Hortensius, T. Zijlstra, J. J. A. Baselmans, S. J. C. Yates, J. R. Gao, and T. M. Klapwijk, *Appl. Phys. Lett.*, **92**, 223502 (2008).
- ¹⁹W. Spengler, R. Kaiser, A. N. Christensen, and G. Müller-Vogt, *Phys. Rev. B*, **17**, 1095 (1978).
- ²⁰S. Doyle, P. Mauskopf, J. Naylor, A. Porch, and C. Duncombe, *J. Low Temp. Phys.*, **151**, 530 (2008).
- ²¹B. O. Johansson, J.-E. Sundgren, J. E. Greene, A. Rockett, and S. A. Barnett, *J. Vac. Sci. Technol. A*, **3**, 303 (1985).
- ²²Z. Dridi, B. Bouhafs, P. Ruterana, and H. Aourag, *J. Phys. Cond. Matt.*, **14**, 10237 (2002).
- ²³W. McMillan, *Phys. Rev.*, **167**, 331 (1968).
- ²⁴E. I. Isaev, S. I. Simak, I. A. Abrikosov, R. Ahuja, Y. K. Vekilov, M. I. Katsnelson, A. I. Lichtenstein, and B. Johansson, *J. Appl. Phys.*, **101**, 123519 (2007).
- ²⁵H. Allmaier, L. Chioncel, and E. Arrigoni, *Phys. Rev. B*, **79**, 235126 (2009).